Supporting Information

Winograd *et al*. 10.1073/pnas.0800360105

SI Experimental Procedures

Slice Preparation. In each of the species, prefrontal cortex was identified as reported in refs. 1–4. Visual cortex slices were obtained from the ferret occipital cortex (5). Somatosensory cortex from the rat was obtained from parasagittal slices (6).

Eletrophysiological Recordings. Sharp intracellular recording electrodes were formed on a Sutter Instruments (Novato, CA) P-97 micropipette puller from medium-walled glass and beveled to final resistances of 50–100 MΩ. Micropipettes were filled with 2 M KAc. Recordings were digitized, acquired, and analyzed using a data acquisition interface and software from Cambridge Electronic Design (Cambridge, U.K.). Data are reported as mean ± SEM.

Drug Application. Drugs were applied either in the bath or locally, through the delivery of a brief pressure pulse (10–150 ms; 100–350 KPa) to a drug-containing micropipette (volumes of 1–20 pl per pulse). The following drugs were used: D-2-amino-5-phosphonopentanoic acid (APV, bath 50 μM), bicuculline methiodide (bath 10 μM), 6-cyano-7-nitroquinoxaline-2,3-dione with 2-hydroxypropyl-β-cyclodextrin) (CNQX-HBC Complex, bath 20 μM) (all from Sigma) and ZD7288 (local 250 μM–1 mM) (TOCRIS).

Calculation of Mean Firing Rate. Mean frequency of firing was calculated in Spike 2 (Cambridge Electronic Design, Cambridge, U.K.). In it, mean frequency is calculated at each event by counting the number of events in the previous period set by the bin size, in our case 1 s. The mean frequency at the current event time is given by:

$$\frac{n-1}{te-t1}\ if\ (te-t1) > \frac{tb}{2}$$

$$\frac{n}{tb}\ if\ (te-t1) \le \frac{tb}{2},$$

where *tb* is the bin size set, *te* is the time of the current event, *t1* is the time of the first event in the time range, and *n* is the number of events in the time range.

Details for Each Voltage-Dependent Current of the Model Neuron. All kinetics below correspond to a temperature of 36°C.

Action Potentials. The voltage-dependent Na^+ current was described by (7):

$$I_{Na} = \bar{g}_{Na} m^3 h (V - E_{Na})$$

$$\frac{dm}{dt} = \alpha_m(V)(1-m) - \beta_m(V)m$$

$$\frac{dh}{dt} = \alpha_h(V)(1-h) - \beta_h(V)h$$

$$\alpha_m = \frac{-0.32(V - V_T - 13)}{\exp[-(V - V_T - 13)/4] - 1}$$

$$\beta_m = \frac{0.28(V - V_T - 40)}{\exp[(V - V_T - 40)/5] - 1}$$

$$\alpha_h = 0.128\exp[-(V - V_T - V_S - 17)/18]$$

$$\beta_h = \frac{4}{1 + \exp[-(V - V_T - V_S - 40)/5]},$$

where $g_{Na} = 70$ mS/cm^2 and $E_{Na} = 50$ mV. $V_T = -55$ mV was adjusted to obtain a spike threshold of around −52 mV.

The "delayed-rectifier" K^+ current was described by (7):

$$I_{Kd} = \bar{g}_{Kd} n^4 (V - E_K)$$

$$\frac{dn}{dt} = \alpha_n(V)(1-n) - \beta_n(V)n$$

$$\alpha_n = \frac{-0.032(V - V_T - 15)}{\exp[-(V - V_T - 15)/5] - 1}$$

$$\beta_n = 0.5\exp[-(V - V_T - 10)/40].$$

Spike-Frequency Adaptation. A slow non-inactivating K^+ current was described by (8):

$$I_{KM} = \bar{g}_{KM} p (V - E_K)$$

$$\frac{dp}{dt} = (p_\infty(V) - p)/\tau_p(V)$$

$$p_\infty(V) = \frac{1}{1 + \exp[-(V + 35)/10]}$$

$$\tau_p(V) = \frac{\tau_{max}}{3.3\exp[(V + 35)/20] + \exp[-(V + 35)/20]},$$

where $g_{KM} = 0.004$ mS/cm^2 and $\tau_{max} = 4$ *s*.

Calcium Currents and Intracellular Calcium Dynamics. A high-threshold Ca^{2+} current was described by (9):

$$I_{CaL} = \bar{P}_{Ca} q^2 G(V, Ca_o, Ca_i)$$

$$\frac{dq}{dt} = \alpha_q(V)(1-q) - \beta_q(V)q$$

$$\alpha_q = \frac{6.32}{1 + \exp[-(V - 5)/13.89]}$$

$$\beta_q = \frac{0.079(1.31 - V)}{1 - \exp[(V - 1.31)/5.36]},$$

where $P_{Ca} = 2.76 \times 10^{-4}$ cm/s is the maximum permeability of the membrane to Ca^{2+} ions, and $G(V,Ca_o,Ca_i)$ is a nonlinear function of voltage and ionic concentrations:

$$G(V, Ca_o, Ca_i) = Z^2F^2V/RT\frac{Ca_i - Ca_o\exp(-ZFV/RT)}{1 - \exp(-ZFV/RT)},$$

where $Z = 2$ is the valence of calcium ions, $F = 96489$ Cmol^{-1} is the Faraday constant, $R = 8.31$ Jmol^{-1}·K^{-1} is the gas constant, and T is the temperature in Kelvin. Ca_i and $Ca_o = 0.002$ M are the intracellular and extracellular Ca^{2+} concentrations (in M), respectively.

Calcium dynamics was handled by a first-order equation to represent calcium buffering and diffusion:

$$\frac{dCa_i}{dt} = \frac{kI_{Ca}}{2Fd} + \frac{Ca_\infty - Ca_i}{\tau_r},$$

where Ca_i is the intracellular calcium concentration, I_{Ca} is the calcium current, $F = 96489$ Cmol^{-1} is the Faraday constant, $d = 1$ μm is the depth of the shell beneath the membrane, and the unit conversion constant is $k = 0.1$ for I_{Ca} in μA/cm^2 and Ca_i in mM. $Ca_\infty = 100$ nM is the equilibrium Ca^{2+} concentration and $\tau_r = 17$ ms is the time constant of calcium removal.

Robustness of the HAGPA Model. The robustness of the model was assessed by changing the values of the different parameters, such as the conductances, their kinetics, and the kinetics of calcium and of calcium regulation of I_h. HAGPA was observed for numerous combinations of these parameters provided that several conditions are met. (*i*) Calcium entry must occur proportional to the firing rate of the neuron; this condition is automatically fulfilled because of the presence of the high-threshold calcium current. (*ii*) The up-regulation of the I_h current occurs for levels of intracellular calcium corresponding to the range of firing rates considered here. The sensitivity of I_h to calcium must be adjusted such that the levels of intracellular calcium are sufficient to activate I_h and also that the calcium level is not too high to avoid saturation of I_h up-regulation (in which case increased persistent firing is observed only for the first pulse). (*iii*) The kinetics of up-regulation of I_h must be slow enough to prevent I_h to recover during the hyperpolarizing pulses. With the slow kinetics identified experimentally in thalamic neurons (10), which correspond to this model, this condition is fulfilled. The range of parameters in which these conditions are met is very broad, and HAGPA can be observed for many combinations of parameters and variations around them (other values than the parameter values listed above can also be used and yield HAGPA of nearly identical characteristics as described in the article). Therefore, rather than a multistable system (11–13), the mechanism that we propose is a continuum of self-sustained states with very slow time constants.

Hyperpolarization-Activated Graded Persistent Activity Starting from a Subthreshold Membrane Voltage Level. We presented in *Results* the phenomenon of HAGPA (hyperpolarization-activated graded persistent activity) as the graded increase in persistent tonic firing occurring as a result of injecting consecutive hyperpolarizing current pulses of the same duration (2–4 s) and amplitude (−0.2 to −0.8 nA). The graded increase in firing frequency had a linear relationship with the number of preceding pulses. As mentioned in the article, in general (35 of 39) HAGPA was evoked only if there was some tonic firing in the neuron (1–4 Hz) at the beginning of the protocol. However, in the remaining neurons (4 of 39), the protocol of hyperpolarizing pulses brought the neuron from a silent, subthreshold state to a suprathreshold, tonic firing mode (Fig. S1 *A* and *B*). In these neurons, a sag is also noticeable during the hyperpolarizing pulse.

Neurons Without Hyperpolarization-Activated Graded Persistent Activity. In *Results*, it was mentioned that a sag was observed during the hyperpolarizing pulses in 37 of 39 neurons that showed HAGPA (Fig. 3*B*). This sag was activated by hyperpolarization and sensitive to blockade with ZD 7288, suggesting that is the result of h-current activation (14, 15). In our sample of 165 neurons, 126 did not show HAGPA, and 39 did. Out of the 126 neurons that did not show HAGPA, 66% showed a sag during hyperpolarizations whereas the remaining 34% did not. From this, we could conclude that the sole presence of a sag during hyperpolarization does not predict that the neuron is going to display HAGPA (see *Discussion*). Additional factors are necessary, and a critical one is that for HAGPA to occur neurons should be able to maintain a tonic firing of action potentials. Indeed, some of the neurons that showed a sag during hyperpolarization (and no HAGPA) could not maintain a tonic firing rate because their action potential firing showed adaptation that silenced the neuron. In Fig. S1*C*, we illustrate an example of a neuron with tonic firing, with no sag during hyperpolarizing pulses and no HAGPA.

Depolarization-suppressed graded persistent activity (DS-GPA) was observed in nine neurons that displayed HAGPA and also in two prefrontal cortex neurons that did not show HAGPA, in three neurons of rat somatosensory cortex and in one neuron of ferret visual cortex, so that the number of neurons in which this phenomenon was observed was $n = 15$.

1. Markowitsch HJ, Pritzel M (1981) Prefrontal cortex of the guinea pig (*Cavia porcellus*) defined as cortical projection area of the thalamic mediodorsal nucleus. *Brain Behav Evol* 18:80–95.
2. Krimer LS, Goldman-Rakic PS (2001) Prefrontal microcircuits: Membrane properties and excitatory input of local, medium, and wide arbor interneurons. *J Neurosci* 21:3788–3796.
3. Trantham-Davidson H, Neely LC, Lavin A, Seamans JK (2004) Mechanisms underlying differential D1 versus D2 dopamine receptor regulation of inhibition in prefrontal cortex. *J Neurosci* 24:10652–10659.
4. Uylings HB, Groenewegen HJ, Kolb B (2003)Do rats have a prefrontal cortex? *Behav Brain Res* 146:3–17.
5. Manger PR, Kiper D, Masiello I, Murillo L, Tettoni L, Hunyadi Z, Innocenti GM (2002) The representation of the visual field in three extrastriate areas of the ferret (*Mustela putorius*) and the relationship of retinotopy and field boundaries to callosal connectivity. *Cereb Cortex* 12:423–437.
6. Paxinos G, Watson C (1998) *The Rat Brain in Stereotaxic Coordinates* (Academic, San Diego).
7. Traub RD, Miles R (1991) *Neuronal Networks of the Hippocampus* (Cambridge Univ Press, Cambridge, UK).
8. Yamada W, Koch C, Adams P (1989) Multiple channels and calcium dynamics. *Methods in Neuronal Modeling*, eds Koch C, Segev I (MIT Press, Cambridge, MA), pp 97–134.
9. McCormick DA, Huguenard JR (1992) A model of the electrophysiological properties of thalamocortical relay neurons. *J Neurophysiol* 68:1384–1400.
10. Luthi A, McCormick DA (1999) Modulation of a pacemaker current through Ca(2+)-induced stimulation of cAMP production. *Nat Neurosci* 2:634–641.
11. Loewenstein Y, Sompolinsky H (2003) Temporal integration by calcium dynamics in a model neuron. *Nat Neurosci* 6:961–967.
12. Teramae JN, Fukai T (2005) A cellular mechanism for graded persistent activity in a model neuron and its implications in working memory. *J Comput Neurosci* 18:105–121.
13. Fransen E, Tahvildari B, Egorov AV, Hasselmo ME, Alonso AA (2006) Mechanism of graded persistent cellular activity of entorhinal cortex layer v neurons. *Neuron* 49:735–46.
14. Harris NC, Constanti A (1995) Mechanism of block by ZD 7288 of the hyperpolarization-activated inward rectifying current in guinea pig substantia nigra neurons in vitro. *J Neurophysiol* 74:2366–2378.
15. Luthi A, Bal T, McCormick DA (1998) Periodicity of thalamic spindle waves is abolished by ZD7288, a blocker of I_h. *J Neurophysiol* 79:3284–3289.
16. Destexhe A, Rudolph M, Fellous JM, Sejnowski TJ (2001) Fluctuating synaptic conductances recreate *in vivo*-like activity in neocortical neurons. *Neuroscience* 107:13–24.

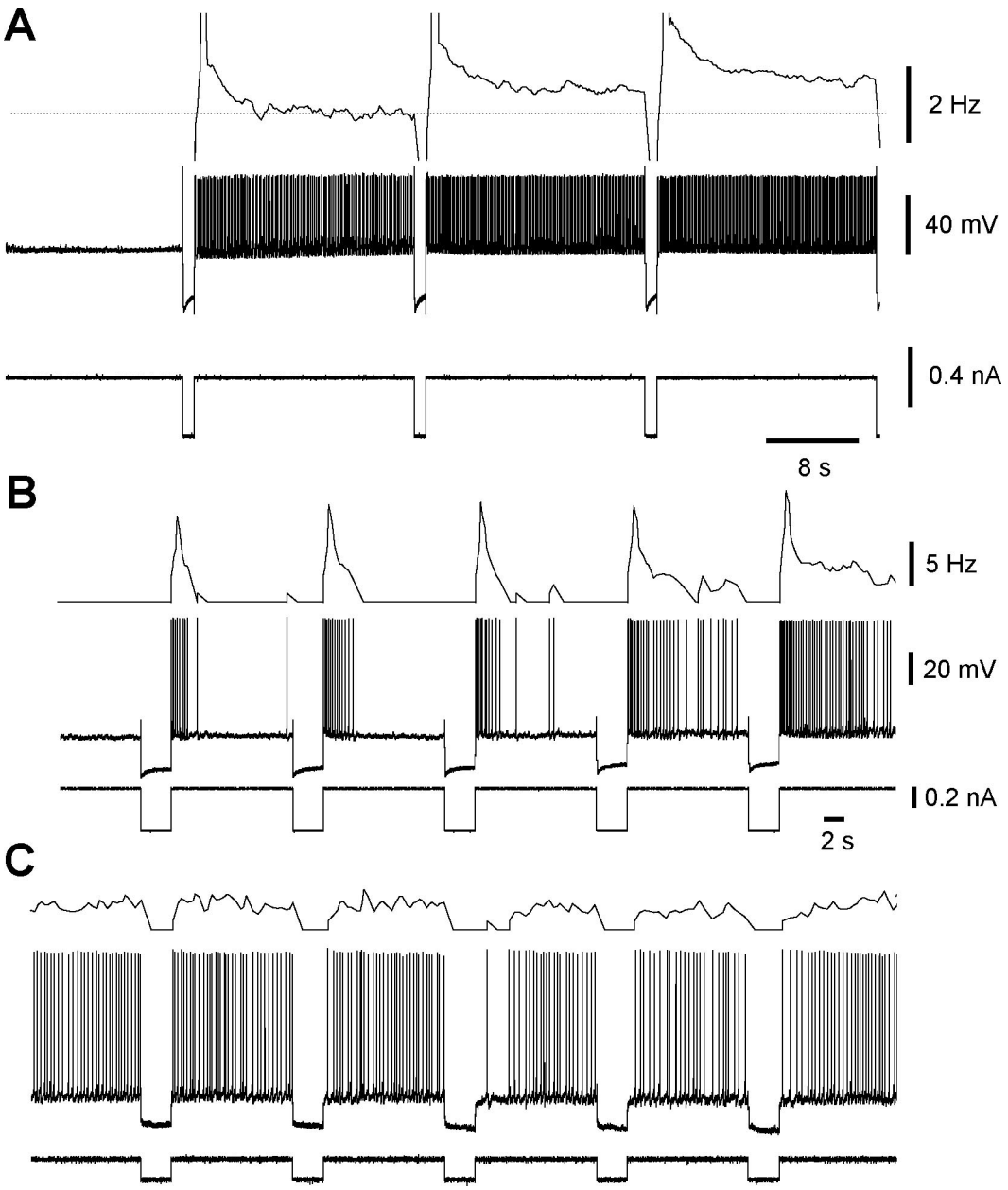

Fig. S1. Neurons with and without hyperpolarization-activated graded persistent activity. (*A*) Example of a neuron that went from a subthreshold membrane potential into tonic firing following the first hyperpolarizing pulse (−0.4 nA, 1 s). The frequency of its tonic firing increased progressively during the successive hyperpolarizing pulses that were given with intervals of 19 s. Mean firing frequency (*Top*) (bin = 1 s), membrane voltage (*Middle*), and intracellularly injected current (*Bottom*). (*B*) Consecutive, equal amplitude hyperpolarizing pulses (−0.4 nA, 3 s) induced a progressive increase in the duration of the rebound discharge following each hyperpolarizing pulse until it generated persistent tonic firing during the 12-s intervals. Note that the neuron is silent before the first hyperpolarizing pulse. Mean firing frequency (*Top*) (bin = 1 s), membrane voltage (*Middle*), and intracellularly injected current (*Bottom*). Note the sag during the hyperpolaring pulses. (*C*) Example of recording from a neuron with neither sag nor HAGPA. Consecutive, equal amplitude hyperpolarizing pulses (−0.2 nA, 3 s) did not induce an increase in the persistent firing rate during the intervals (12 s). Pulses of more intensity did not induce HAGPA either (not shown). Firing frequency rate (*Top*) (bin = 1 s), membrane voltage (*Middle*), and intracellularly injected current (*Bottom*). Note the absence of sag during the hiperpolarizing pulse. *A*, *B*, and *C* correspond to different neurons.

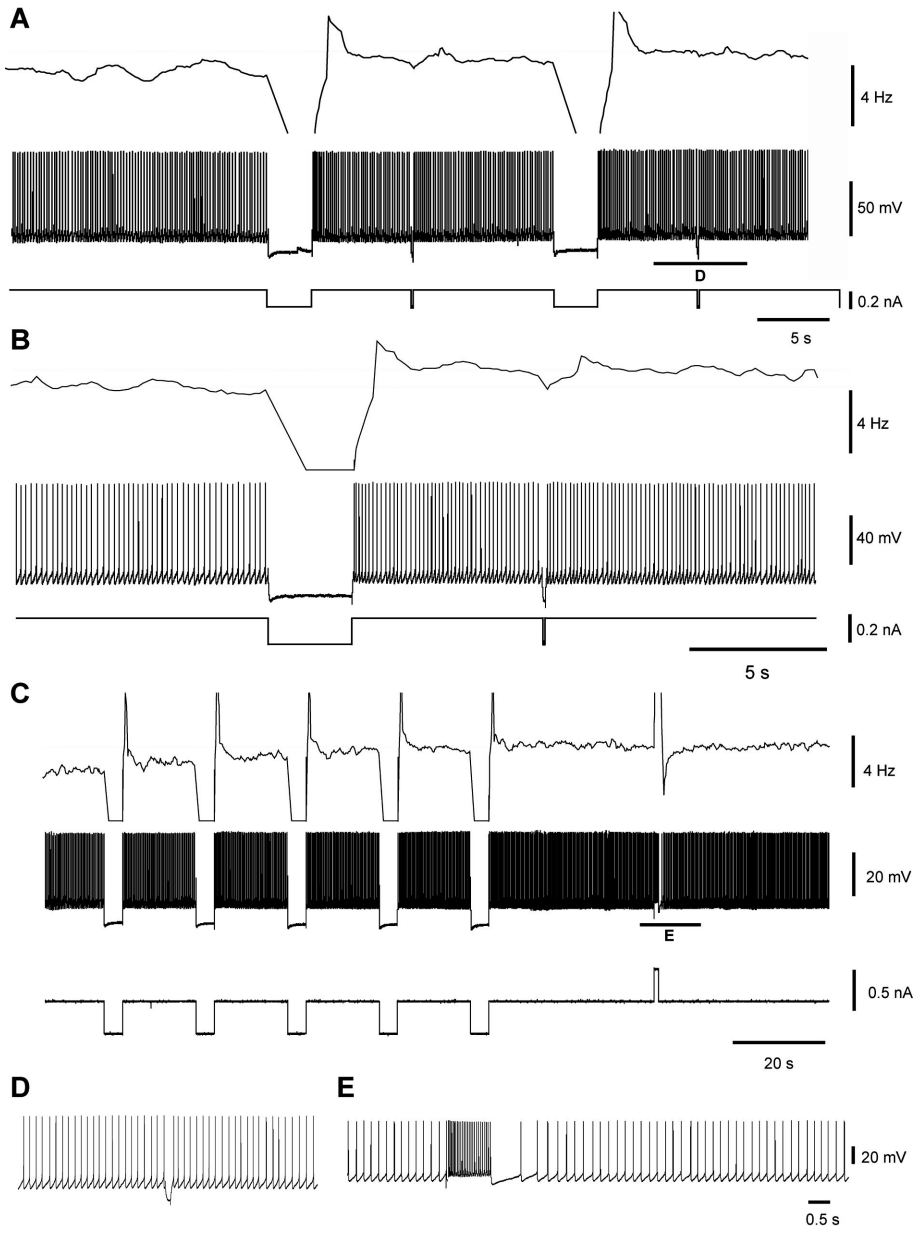

Fig. S2. Stability of action potential firing frequency in the presence of disturbances. (*A*) HAGPA protocol (hyperpolarizing pulses −0.2 nA, 3 s) in a neuron exhibiting an initial firing frequency of 5.6 Hz (*Left*). During the second and third intervals a short hyperpolarizing pulse (−0.2 nA, 120 ms) was given, with no detectable effect in the firing frequency. The underlined area of the recording is expanded in *D*. Shown are mean firing frequency (*Top*) (bin = 1 s), membrane voltage (*Middle*), and intracellularly injected current (*Bottom*). (*B*) A different example is shown for another neuron. The first hyperpolarizing pulse is of −0.3 nA and 3 s duration, and the second one is of the same amplitude and lesser duration (120 ms). Note how the long hyperpolarizing pulse induces an increase in the mean firing frequency whereas the short one does not. (*C*) A different example of an HAGPA protocol, illustrating the gradual increase in mean firing frequency. The purpose of this panel is to illustrate the stability of the increased firing at the end of the protocol for 73 s. It is also useful to illustrate the stability of the firing even in the presence of a short depolarizing pulse (0.4 nA, 1 s). The underlined area is expanded in *E*. (*D*) Expanded trace underlined in *A*. (*E*) Expanded trace underlined in *C*.

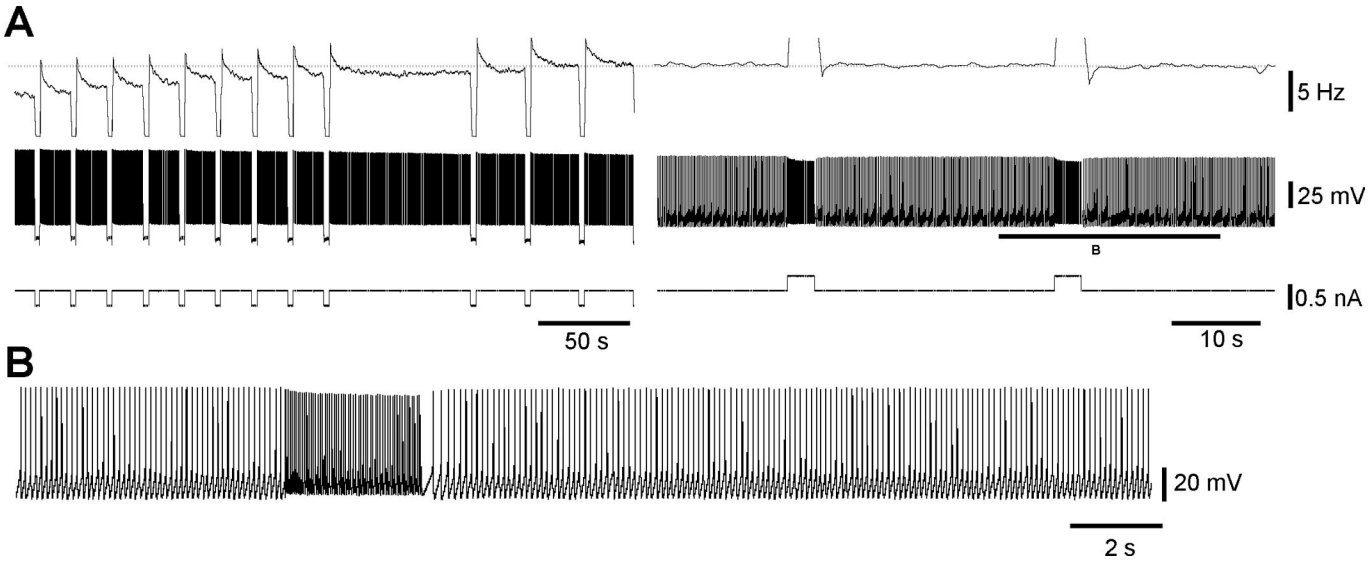

Fig. S3. Neuron with HAGPA and no DGSPA. (*A*) HAGPA protocol generated by hyperpolarizing current injection (−0.3 nA, 3 s) with intervals of 17 s. In the middle of the protocol, a longer interval (78 s), to explore stability of firing frequency. Note how the firing remained stable at 7.8 Hz, and kept increasing when more hyperpolarizing pulses were given. At the end of the protocol, and starting from the final reached frequency (8.8 Hz) two depolarizing pulses were given (−.3 nA, 3 s) without producing any change in the firing frequency. Shown are mean firing frequency (*Top*) (bin = 1 s), membrane voltage (*Middle*), and intracellularly injected current (*Bottom*). The underlined trace is expanded in *B*. Recordings from the same neuron were displayed in Fig. 1*B*.

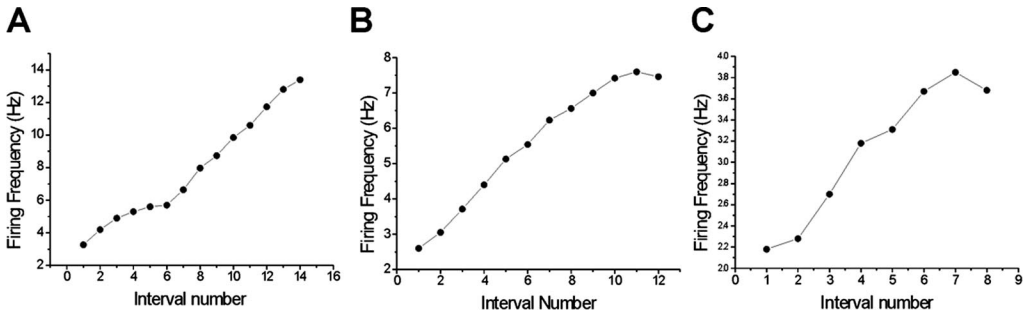

Fig. S4. Firing frequency plateau following a HAGPA protocol. (*A*) Example of the progressive increase in the firing frequency during consecutive intervals between hyperpolarizing pulses (−0.3 nA, 2 s). This neuron does not reach a plateau in the firing frequency (13.4 Hz) until the 14th interval. (*B*) Example of a neuron that reached a firing frequency plateau after 10 intervals. The maximum frequency was 7.4 Hz (pulses were of −0.5 nA and 3 s.). (*C*) Example of increase in firing frequency for a different neuron, which reached a firing plateau after six intervals, the plateau being of 3.7 Hz (pulses were of −0.5 nA and 3 s.)

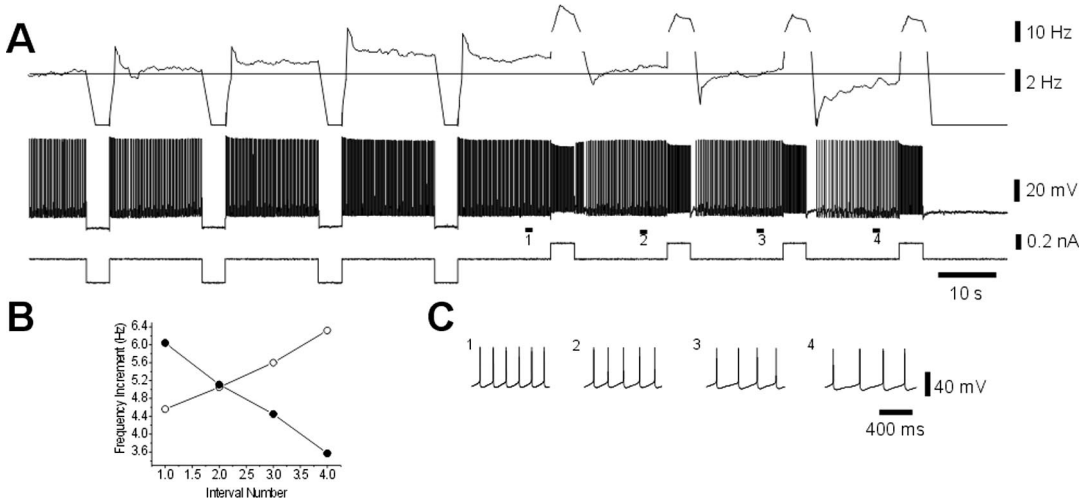

Fig. S5. Consecutive hyperpolarization-activated increase in firing frequency (HAGPA) and depolarization-suppressed graded persistent activity (DSGPA). (*A*) Following four hyperpolarizing pulses of an HAGPA protocol (−0.3 nA, 4s), inverse, depolarizing pulses (0.2 nA, 4 s) were given. The progressive increase in firing frequency induced by the HAGPA protocol was reverted by the inverse protocol (DSGPA). In the case illustrated, the firing frequency at the end of the HAGPA protocol was 6 Hz, and after four consecutive depolarizing pulses the neuron was silenced. (*Top* to *Bottom*) Rate of spike frequency (bin = 1 s; *Top*), membrane voltage, and intracellular injected current. (*B*) Firing frequency during the interval versus interval number for HAGPA (○) and DSGPA (●) protocols. (*C*) Expanded traces of membrane potential corresponding to the indicated time periods (1–4) for the DSGPA protocol are shown to better illustrate the decrease in the firing frequency.

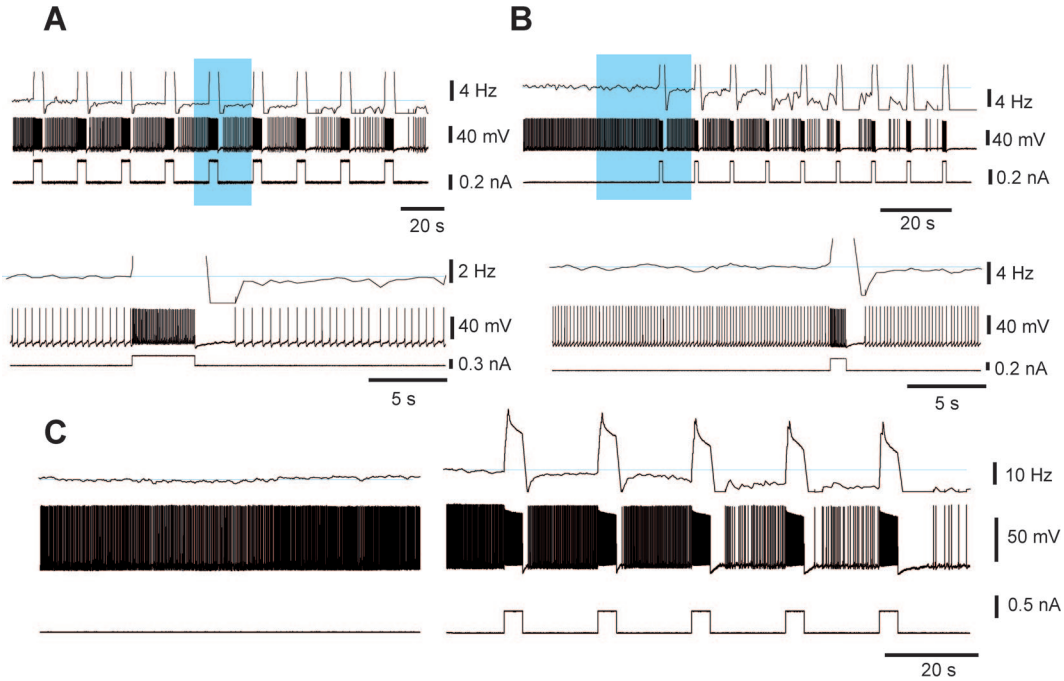

Fig. S6. Three different examples of DSGPA and stability of firing. (*A*) DSGPA induced by consecutive depolarizing pulses of (0.3 nA, 4 s) with intervals of 16 s. This protocol led the tonic firing from 3.1 Hz to 1 Hz at the end (right hand side). The area highlighted in blue is expanded in the panel below. As in previous figures, the traces are: mean frequency (bin 1 s) (*Top* trace), membrane potential (*Middle* trace), intracellularly injected current (*Bottom* trace). (*B*) A different neuron, firing tonically at 5.2 Hz, 38 s is displayed to illustrate the stability of the firing. Nine consecutive pulses (0.3 nA, 1 s) manage to silence the neuron. Highlighted area is expanded in the panel below. (*C*) Continuous firing of a neuron at 6.35 Hz for 82 s. After an interval of 40 s, which is not displayed, five consecutive pulses of 0.5 nA and 4 s were given, decreasing the tonic firing frequency from 8.8 to 1 Hz.

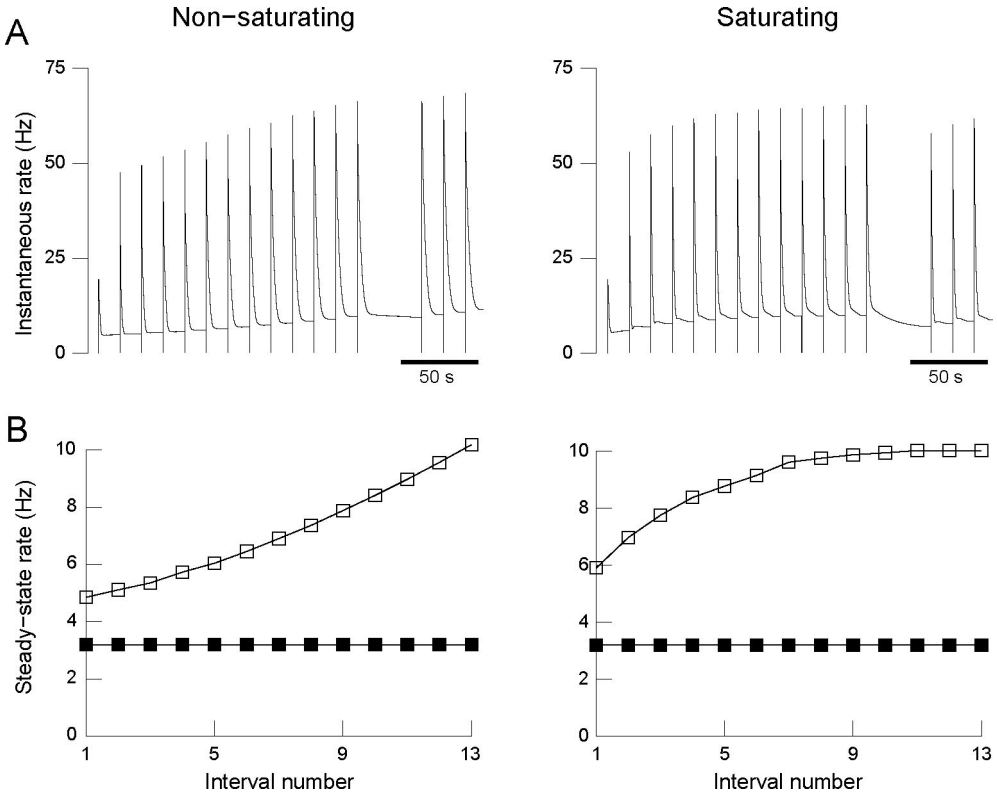

Fig. S7. Two types of convergence to steady-state in the model. (*A*) Instantaneous firing rate in a similar protocol as in Fig. 4*B* (the *Left* panel here is identical to Fig. 4*B*). (*B*) Increment in spike frequency during the steady state in the interval versus interval number the HAGPA protocol in *A* (□) and during the same protocol but in the absence of I_h (■). The model is shown for two different parameter sets. (*Left*) In control conditions, the model is said to be ''Non-saturating'' because the firing rate does not converge to a stable value for typical experimental protocols (i.e., a few minutes of recording). Note that, in fact, the rate saturates at a longer time scale (not shown). (*Right*) Other model parameters (for the I_h regulation by calcium; $k_2 = 0.0001\ ms^{-1}$, $k_4 = 0.008\ ms^{-1}$) give rise to a ''Saturating'' model. Here, the rate saturates to a stable value after a few successive intervals.

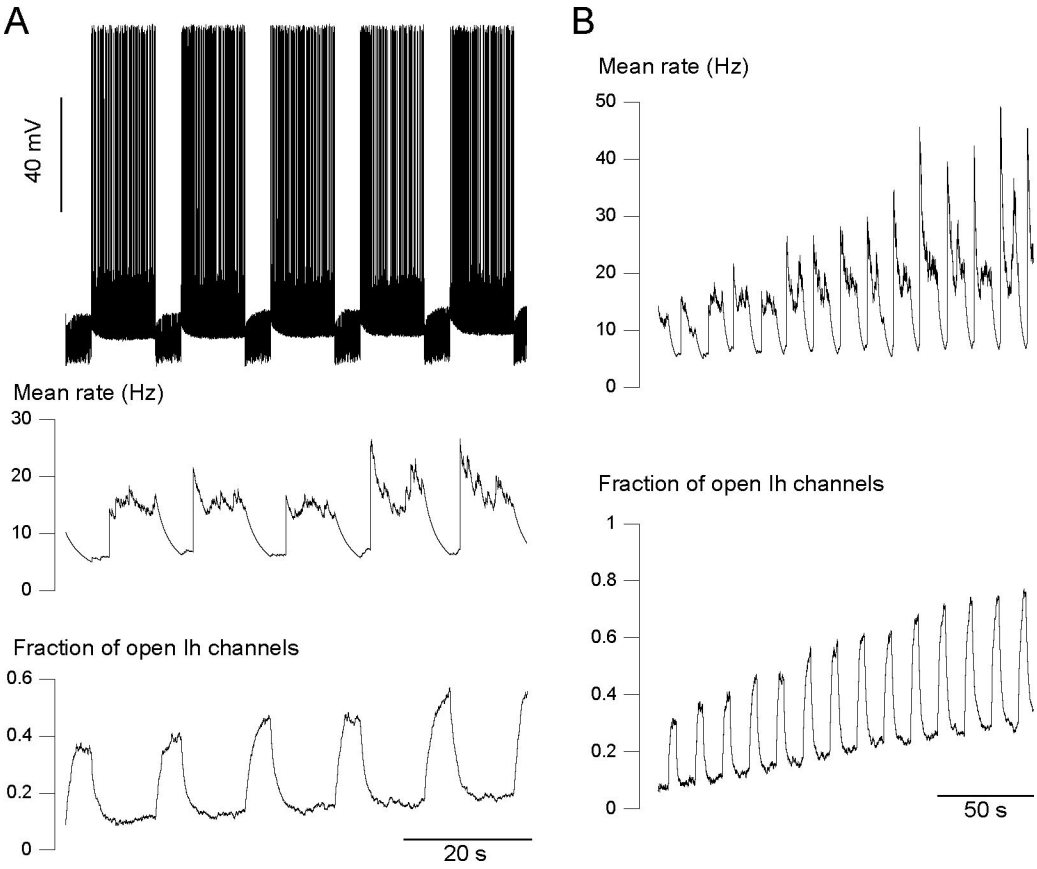

Fig. S8. Model of HPGA with synaptic inputs. (*A*) HAGPA with simulated synaptic bombardment consisting of mixed random excitatory and inhibitory inputs (model adapted from ref. 16). In the hyperpolarized phases, the synaptic inputs were dominated by inhibition (g_e0 = 0.5 nS; sigma_e = 0.1 nS; g_i0 = 10 nS; sigma_i = 2 nS), whereas during the depolarized phase, it was dominated by excitation (g_e0 = 1.5 nS; sigma_e = 2.5 nS; g_i0 = 0.5 nS; sigma_i = 0.2 nS). (*Top*) Membrane potential. (*Middle*) Instantaneous firing rate. (*Bottom*) Fraction of open I_h channels. (*B*) Instantaneous firing rate (*Top*) and open I_h channels (*Bottom*) at a longer time scale in the same simulation as in *A*.

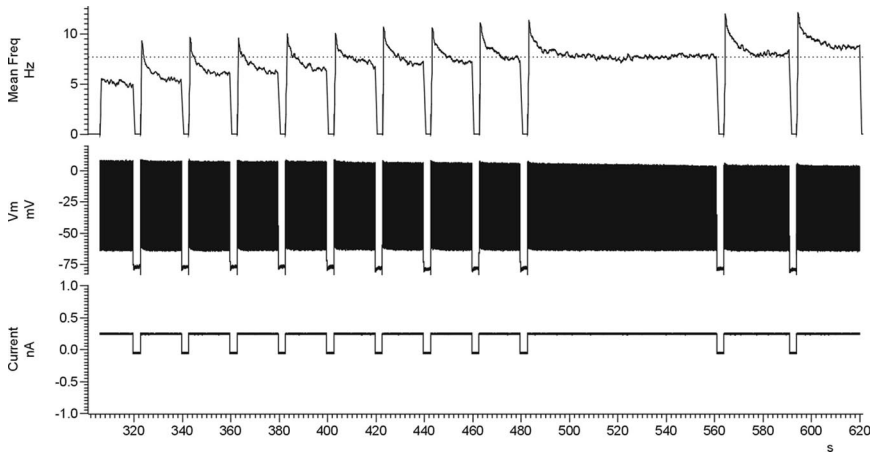

Movie S1. Intracellular recordings from neurons that illustrate the phenomena being reported in this article. The neuron displayed in HAGPA is the same as that in Fig. 1*B*. (*Top*) Mean frequency of discharge (Hz). (*Middle*) Membrane potential (mV). (*Bottom*) Current intracellularly injected into the cell.

Movie S1 (MOV)

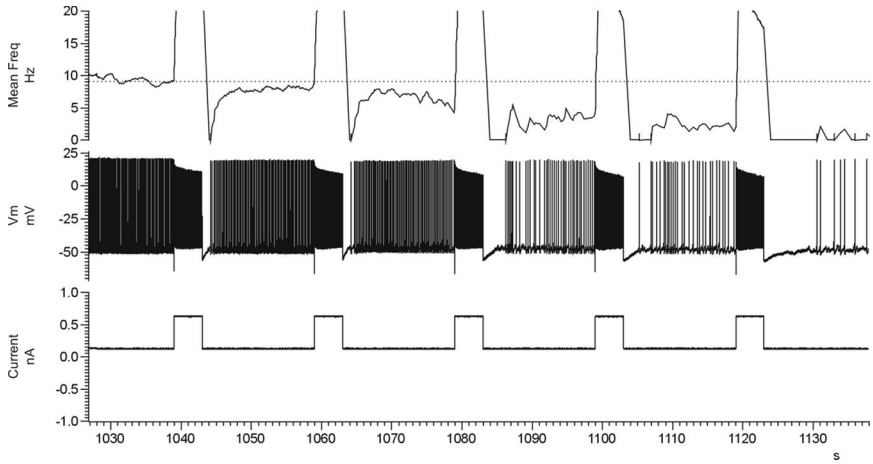

Movie S2. Intracellular recordings from neurons that illustrate the phenomena being reported in this article. The neuron displayed in DSGPA is a neuron recorded in supragranular layers from ferret prefrontal cortex. (*Top*) Mean frequency of discharge (Hz). (*Middle*) Membrane potential (mV). (*Bottom*) Current intracellularly injected into the cell.

Movie S2 (MOV)